An Intermediate State of the γ-Aminobutyric Acid Transporter GAT1 Revealed by Simultaneous Voltage Clamp and Fluorescence

Ming Li, Robert A. Farley, and Henry A. Lester

From the Division of Biology, California Institute of Technology, Pasadena, California 91125

abstract   The rat γ-aminobutyric acid transporter GAT1 expressed in *Xenopus* oocytes was labeled at Cys74, and at one or more other sites, by tetramethylrhodamine-5-maleimide, without significantly altering GAT1 function. Voltage-jump relaxation analysis showed that fluorescence increased slightly and monotonically with hyperpolarization; the fluorescence at −140 mV was ∼0.8% greater than at +60 mV. The time course of the fluorescence relaxations was mostly described by a single exponential with voltage-dependent but history-independent time constants ranging from ∼20 ms at +60 mV to ∼150 ms at −140 mV. The fluorescence did not saturate at the most negative potentials tested, and the midpoint of the fluorescence–voltage relation was at least 50 mV more negative than the midpoint of the charge–voltage relation previously identified with Na^+ binding to GAT1. The presence of γ-aminobutyric acid did not noticeably affect the fluorescence waveforms. The fluorescence signal depended on Na^+ concentration with a Hill coefficient approaching 2. Increasing Cl^- concentration modestly increased and accelerated the fluorescence relaxations for hyperpolarizing jumps. The fluorescence change was blocked by the GAT1 inhibitor, NO-711. For the W68L mutant of GAT1, the fluorescence relaxations occurred only during jumps to high positive potentials, in agreement with previous suggestions that this mutant is trapped in one conformational state except at these potentials. These observations suggest that the fluorescence signals monitor a novel state of GAT1, intermediate between the E^*_{out} and E_{out} states of Hilgemann, D.W., and C.-C. Lu (1999. *J. Gen. Physiol.* 114:459–476). Therefore, the study provides verification that conformational changes occur during GAT1 function.

key words: voltage clamp • *Xenopus* oocyte • tetramethylrhodamine • conformational change

INTRODUCTION

Specific Na^+-coupled transporters are present on neuronal and glial membranes for all known low–molecular weight neurotransmitters or, in the case of acetylcholine, for their catabolites. These transporters are thought to be responsible for removal of the neurotransmitter from the vicinity of receptors and are therefore important for termination of synaptic transmission. To influence the time course of synaptic transmission, this removal would be expected to occur on a time scale of milliseconds for ligand-gated channels, and on a time scale of hundreds of milliseconds for G-protein–coupled receptors. This postulated role for neurotransmitter transporters in neurotransmission calls for direct measurements of the time course of neurotransmitter transporter action.

Besides their postulated physiological function, neurotransmitter transporters are pharmacologically important: they appear to be the sites of action for important abused (cocaine) and therapeutic (antidepressants, psychostimulants, antiepileptics) drugs (Kuhar et al., 1991; Amara and Kuhar, 1993; Lester et al., 1996). Despite their pharmacological function, the molecular mechanisms of these inhibitors are not known. Understanding the detailed mechanism of neurotransmitter transporter action would facilitate rational drug design.

Therefore it is an important goal to study the physical mechanism of neurotransmitter transporters at the molecular level. The driving force for transporting neurotransmitter across the cell membrane comes from the electrochemical gradient of the cotransported ions, primarily Na^+. Na^+, Cl^-, and sometimes K^+ are cosubstrates with a stoichiometry of 1 or 2 mol/mol of neurotransmitter (Rudnick, 1977; Kanner, 1978; Rudnick and Nelson, 1978; Kanner and Bendahan, 1982; Pastuszko et al., 1982; Radian and Kanner, 1983, 1985). With the molecular cloning of the γ-aminobutyric acid (GABA) transporter GAT1 (Guastella et al., 1990), and the subsequent cloning of many other neurotransmitter transporters (Blakely et al., 1991; Hoffman et al., 1991; Pacholczyk et al., 1991; Shimada et al., 1991; Usdin et al., 1991), research on neurotransmitter transporters has been accelerating. Sequence analysis shows that some neurotransmitter transporters, such as GAT1 and the serotonin transporter SERT, are homologous members of a family whose members are postulated to contain 12 transmembrane helices and ∼600 amino acid residues. Structure–function studies of transporters in this GAT1 family, based on site-directed mutagenesis and heterologous expression, have

Address correspondence to Henry A. Lester, Division of Biology 156-29, California Institute of Technology, 1201 East California Boulevard, Pasadena, CA 91125. Fax: 626-564-8709; E-mail: lester@caltech.edu

identified certain residues that are critical for transporter function and have provided clues about some functional domains (Mabjeesh and Kanner, 1992; Bendahan and Kanner, 1993; Pantanowitz et al., 1993; Kleinberger-Doron and Kanner, 1994; Penado et al., 1998). Nevertheless, the actual molecular structure and physical mechanism(s) of transport is still not known. This situation calls for additional biophysical study of these transporters.

In this research, we used combined electrophysiological and optical techniques to study the molecular mechanism of neurotransmitter transporter function. Electrophysiology can be used for transporter studies because ion binding and translocation steps, which are partial reactions in the transport cycle, produce electrical signals. For GAT1, electrophysiology is employed to assess rates, reaction steps, and turnover numbers (Mager et al., 1993, 1996; Hilgemann and Lu, 1999; Lu and Hilgemann, 1999a,b). On the other hand, recording of fluorescent probes has more recently been applied to monitor the conformational changes of channel proteins (Mannuzzu et al., 1996; Cha and Bezanilla, 1997, 1998; Siegel and Isacoff, 1997; Baker et al., 1998; Loots and Isacoff, 1998) and transporters (Loo et al., 1998) expressed in cell membranes. Such experiments have provided important insights into the motion of S2 and S4 segments of K^+ channel domains and the Na^+-glucose transporter.

For the experiments, we built an apparatus for simultaneous electrophysiological and optical recording from *Xenopus* oocytes. We detected and analyzed conformational transitions at GAT1 with a time resolution of milliseconds. These results may contribute to explaining the molecular mechanism of transporter function and drug action, which are important for understanding the physiological and pathological role of neurotransmitter transporters in native cells.

Our studies were enhanced by the use of two previously characterized GAT1 mutants. (a) The C74A mutant functions rather similarly to wild type (WT),[1] yet is insensitive to the sulfhydryl reagent MTS-ethyltrimethylammonium (MTSET) (Yu et al., 1998). This mutant was therefore expected to undergo normal conformational changes, but to lack a crucial site for labeling by sulfhydryl-specific probes. Indeed, we find that C74A-GAT1 is labeled to a lesser extent than WT-GAT1 by our fluorescent probe, tetramethylrhodamine maleimide. (b) The W68L mutant appears to be locked in a high-affinity state for Na^+ (Mager et al., 1996). We expected that this W68L-GAT1 would show WT levels of labeling but reduced fluorescence relaxations. This expectation is fulfilled.

Reagents and Solutions

The fluorescent dye tetramethylrhodamine-5-maleimide was purchased from Molecular Probes, Inc. The blocking reagent 3-maleimidopropionic acid was purchased from Aldrich Chemical Co. MTSET was purchased from Toronto Research Chemicals. The GAT1 inhibitor NO-711 was purchased from Research Biochemicals, Inc. Other reagents were purchased from Sigma Chemical Co. The recording solution, ND96, contained 96 mM NaCl, 2 mM KCl, 1 mM $MgCl_2$, and 5 mM HEPES, pH 7.4. The incubation solution contained ND96 plus 2% horse serum. The NMDG substitution for Na^+ contained 96 mM NMDG instead of Na^+ in the ND96 solution. The gluconate substitution of Cl^- contained 96 mM gluconate instead of Cl^- in the ND96 solution.

Oocyte Expression

The high-efficiency expression system for GABA and serotonin transporters in *Xenopus* oocytes (Mager et al., 1993) was used for rGAT1 expression, with modifications for the fluorescence labeling. In brief, 30 ng cRNA of WT-rGAT1 (Mager et al., 1993) or C74A-rGAT1 (Yu et al., 1998) was injected into stage VI oocytes and the cells were incubated at 18°C for 1 d, and then moved to 12°C for incubation for 5 d. At the end of the sixth day of incubation, the oocytes were treated for fluorescence labeling, as described in the following.

Fluorescence Labeling and MTSET Reaction

At the end of the sixth day of incubation, the oocytes were reacted with 10 mM 3-maleimidopropionic acid in ND96 for 1 h at 18°C, to block the endogenous reactive sulfhydryl groups in the oocyte membrane. After this blocking reaction, the oocytes were washed and brought to 18°C incubation for 1 d. On the eighth day after cRNA injection, the oocytes were incubated in ND96 solution containing 5 mM tetramethylrhodamine-5-maleimide (TMRM) for 1 h on ice as described (Mannuzzu et al., 1996), or at room temperature for 30 min; these two treatments produced similar results in the fluorescence signals. The labeled oocytes were then washed and incubated in ND96, ready for recording and GABA uptake assay. For MTSET reactions, oocytes were incubated in ND96 containing 3.75 mM MTSET for 0.5 h at room temperature (Yu et al., 1998).

The result of TMRM labeling was examined by measuring the fluorescence intensity of the oocyte surface at the animal pole with the apparatus described below, and by fluorescence confocal imaging of the oocyte surface using a MRC-600 confocal microscope (MRC-600; Bio-Rad Laboratories) with a 10×, NA 0.5 objective.

Apparatus

The recording setup, as shown in Fig. 1, consists of a microscope, a photomultiplier tube (PMT) attached to the side port of the microscope, and conventional two-electrode voltage clamp instruments. The inverted fluorescence microscope (IX-70-FLA; Olympus Corp.) is fitted with a stabilized 100-W Hg light source and an oil-immersion objective of 40×, NA 1.3. The dichroic mirror is the high Q TRITC set from Chroma Technology Corp. The PMT (R928P; Hamamatsu Phototonics) is in a housing originally built by Photon Technology, Inc. The oocyte is placed on the microscope stage and is visualized for electrophysiology by a separate stereomicroscope. The exciting beam was attenuated by factors approaching 300 by neutral density filters; therefore, an incandescent lamp would probably suffice. A digitally controlled (i.e., finger-operated) shutter blocked the beam, except during actual data trials, to minimize bleaching. The emission signal from the oocytes was appropriately amplified and filtered at 200
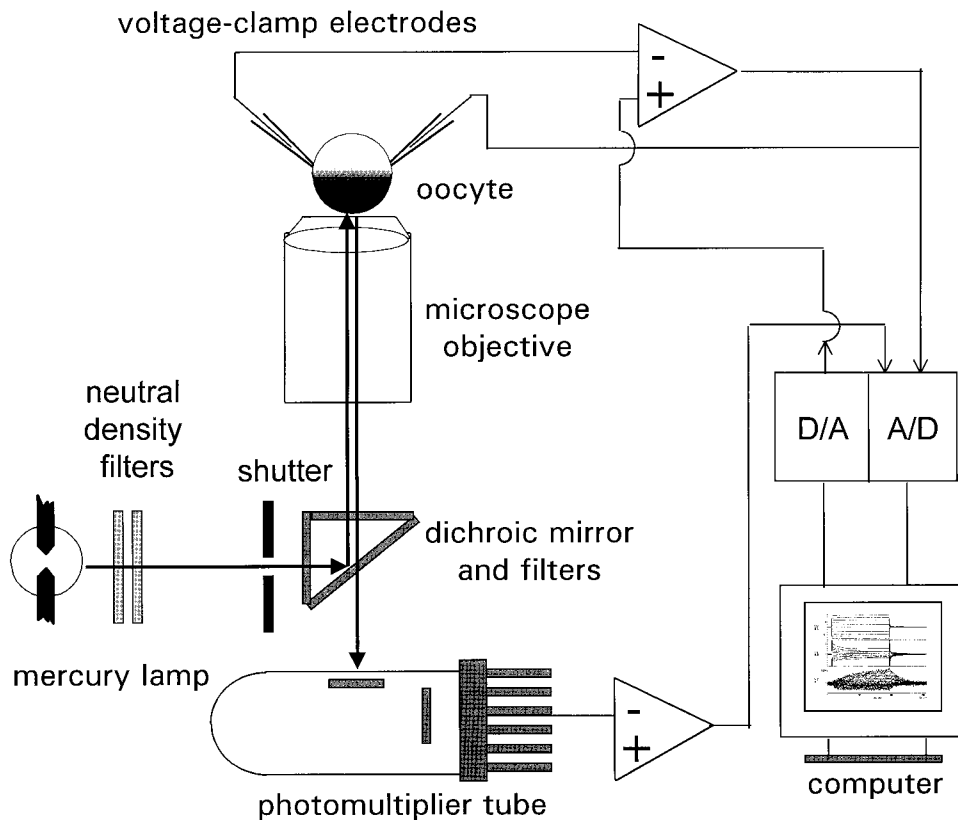
Figure 1. Instrumentation for measuring fluorescence from voltage-clamped oocytes. The recording apparatus consists of a microscope (depicted by the objective and dichroic mirror), a photomultiplier tube attached to the side port of the microscope, and conventional two-electrode voltage-clamp instruments. The apparatus uses a stabilized 100-W Hg light source coupled to an inverted microscope (IX-70; Olympus Corp.), dichroic filter cubes for delivering the light, a 40× objective lens, and a photomultiplier tube to collect the fluorescence emission. The oocyte is placed on the microscope stage with its animal pole facing down and is visualized for electrophysiology by a separate stereomicroscope (not shown). The exciting beam is attenuated by factors approaching 300. The emission signal from the oocytes is collected by the objective lens and sent to the PMT. Appropriate amplifiers and electronic filters condition the signal. The command and output signals are interfaced with a computer through A/D and D/A converters.

Hz by an eight-pole low-pass filter (902-LPF; Frequency Devices, Inc.). Each trace was acquired and averaged over 30 sweeps by an Axon Digidata interface and pCLAMP 7 (Axon Instruments). A HumBug (Quest Scientific) removed the remaining 60 Hz. Two-electrode voltage clamp procedures were used as described (Quick and Lester, 1994; Mager et al., 1998). We optimized the apparatus using the *Shaker* H4 R359C mutation, generously provided by E. Isacoff (Univerisity of California, Berkely, Berkely, CA), and found 31% changes in fluorescence upon voltage depolarization from −80 to +40 mV. This signal is comparable with previous results with a similar apparatus (Mannuzzu et al., 1996).

Off-line Data Analysis

Steady state fluorescence values were measured as the average over the final 200 ms at the test potential. For kinetic analyses such as those shown in Figs. 6–9 (below), signals were subjected to further averaging across cells, digital filtering (50 Hz eight-pole Bessel), baseline alignment, and linear detrending where appropriate. Waveforms were fit to single or double exponentials with routines in ORIGIN 5 and CLAMPFIT 8. In preliminary analyses, we verified that (a) the baseline alignment did not result in systematic voltage-dependent shifts, and (b) the linear detrending did not result in systematic elimination of slow exponential components with time constants of ~500 ms or less. We cannot rule out the possibility that relaxations with larger time constants would be detected by test potentials longer than those used here.

Because the fluorescence relaxations were small and noisy, accurate analysis of these relaxations is a major topic of this paper. Therefore, several details of the analysis are evaluated in the results. Figs. 5 and 6 show the progression from raw to analyzed traces for two important data sets. Figs. 7 and 8 present tests for history dependence. Figs. 9 and 10 compare two methods for analyzing the voltage dependence of the fluorescence relaxations.

GABA Uptake Assay

[3H]GABA uptake experiments were performed as follows. Oocytes expressing GAT1 were incubated in ND96 solution containing various concentrations of GABA and trace amounts of [3H]GABA for 20 min, and then washed with ND96 solution five times. Each individual oocyte was then dissolved in 1 ml 10% SDS and the radioactivity was measured using a scintillation counter (LS 5000 TD/TA; Beckman Instruments Inc.).

R E S U L T S

TMRM Treatment of GAT1 Does Not Affect GABA Uptake

Fig. 2 presents results of [3H]GABA uptake experiments on oocytes expressing WT-GAT1 and exposed either to TMRM or MTSET. TMRM labeling did not significantly affect GABA uptake: for eight cells measured at 128 mM extracellular GABA, the uptake was 0.32 ± 0.02 and 0.33 ± 0.02 pmol/oocyte per 20 min in unlabeled and TMRM-labeled oocytes, respectively. When the data in Fig. 2 were fit by hyperbolic (or Michaelis-Menten) dose–response relations, the unlabeled and TMRM-labeled oocytes yielded virtually identical values: $K_m = 83 \ \mu M$ and $V_{max} = 0.54$ pmol/oocyte per 20 min. These K_m values are several times higher than the values previously observed for GAT1 expressed in oocytes (Guastella et al., 1990). One possible explanation for this observation is that the prolonged incubation (7 d) followed by reaction with maleimidopropionic acid (the preblocking step) increases the intracellular Na^+ and/or Cl^-
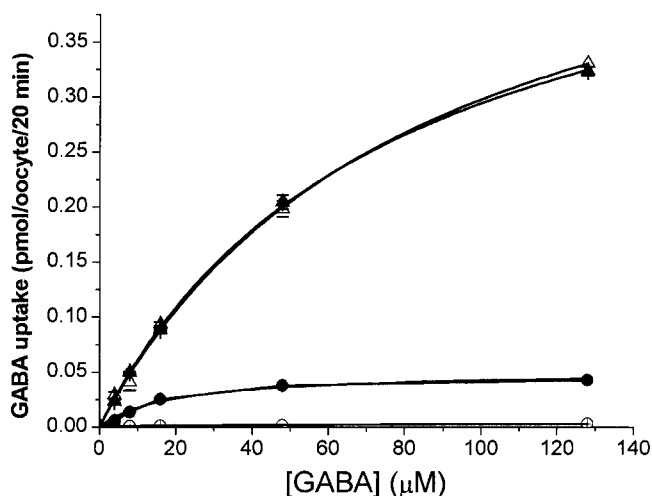
Figure 2. [³H]GABA uptake assayed in oocytes expressing WT-GAT1[7]. The GABA uptake activity was measured in uninjected (○), GAT-1 mRNA-injected (△), GAT-1 mRNA-injected and TMRM-labeled (▲), and GAT-1 mRNA-injected and MTSET-treated (●) oocytes. Each data point is the mean value of measurements from three to four cells, and the error bars indicate SEM. The curves are the nonlinear fits to hyperbolic dose–response relations (Michaelis-Menten equation).

concentration and thereby increases the K_m for GABA (Lu and Hilgemann, 1999b). This preblocking step was done for both unlabeled and TMRM-labeled oocytes.

GAT1 and C74A-GAT1 Are Labeled by TMRM

Fluorescent labeling of GAT1 by TMRM was verified by confocal microscopy (Fig. 3) and was quantified by PMT measurements of the fluorescence of the oocyte surface at the animal pole, where the autofluorescence was partially absorbed by the pigment granules. We also studied C74A-GAT1, a mutant that is less susceptible to sulfhydryl reagents (Yu et al., 1998). The results are shown in Table I. It is clear that oocytes expressing either C74A or WT-GAT1 were labeled more than uninjected oocytes; furthermore, WT-GAT1 displayed higher fluorescence than C74A (10.6 versus 6.4 V PMT signal, respectively). As shown below, the C74A mutant displays the same maximal function as WT-GAT1 when expressed in oocytes; therefore, the reduced labeling of C74A is probably not caused by reduced expression levels. It is most likely that elimination of the cysteine at position 74 decreases the labeling by the cysteine-specific reagent TMRM. We conclude that Cys74 is labeled by TMRM in WT-GAT1, in addition to at least one other site that is labeled in both WT-GAT1 and the C74A mutant.

TMRM Labeled WT-GAT1 and C74A-GAT1 Have Very Similar Electrophysiological Properties

Fig. 2 showed that reaction with TMRM had little effect on GABA uptake by GAT1. We also found only small reductions in GABA-induced currents in electrophysio-
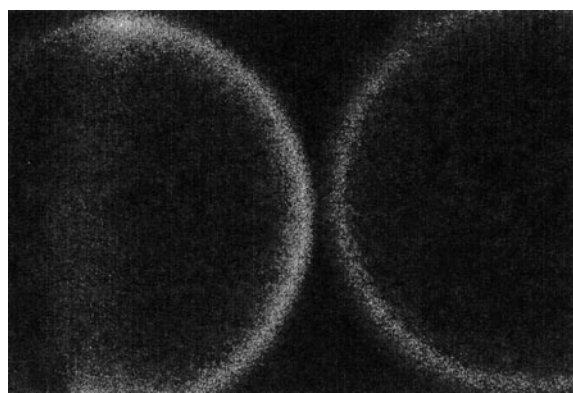

Figure 3. Confocal microscopy of *Xenopus* oocytes labeled with tetramethylrhodamine as described in materials and methods. (Left) Injected with WT-GAT1, (right) uninjected. The oocytes are 0.9 mm in diameter. The more intense fluorescence is at the animal pole.

logical studies. In measurements of transport-associated currents (200 μM GABA, −60 mV, measured at the end of a 40-s application), exposure to TMRM decreased currents by 17 ± 18% for WT-GAT1 and by 17 ± 5% for C74A-GAT1 (mean ± SEM, $n = 7$ and 2, respectively). Fig. 4 presents additional data on electrophysiological properties of TMRM-labeled WT-GAT1 and C74A-GAT1. Fig. 4 A shows that the time course and amplitude of GABA-induced current are quite similar. Average WT-GAT1 and C74A GABA-induced currents (100 μM, −60 mV, 40-s application) in the experiments of Fig. 4 A were 120 ± 27 and 140 ± 42 nA, respectively (mean ± SEM, $n = 8$).

We also compared charge movements during voltage-jump relaxations in the absence of GABA for uninjected oocytes, WT-GAT1-injected oocytes, and C74A-injected oocytes. After each jump, the oocytes expressing WT-GAT1 and C74A display transient currents, which relax to new steady state currents over a time course of hundreds of milliseconds. The transient currents have previously been analyzed in detail (Mager et al., 1993, 1996; Hilgemann and Lu, 1999; Lu and Hilgemann, 1999a,b). Examples of the traces will be shown in Fig. 5 (below). The time integral of the transient current is interpreted as the reversible binding of Na⁺ to GAT1 in the absence of GABA (Mager et al., 1993, 1996). This integral is plotted against membrane potential in Fig. 4 B, and the data are fit to the Boltzmann

TABLE I
Fluorescence Intensity of Oocyte Membrane

Sample	Uninjected	C74A-injected	WT-injected
Fluorescence intensity, V	2.1 ± 0.1	6.4 ± 0.6	10.5 ± 0.5

Fluorescence intensity was measured as the output from the photomultiplier tube at a working voltage of 700 V, after 100× amplification. All data are mean ± SEM ($n = 7$).
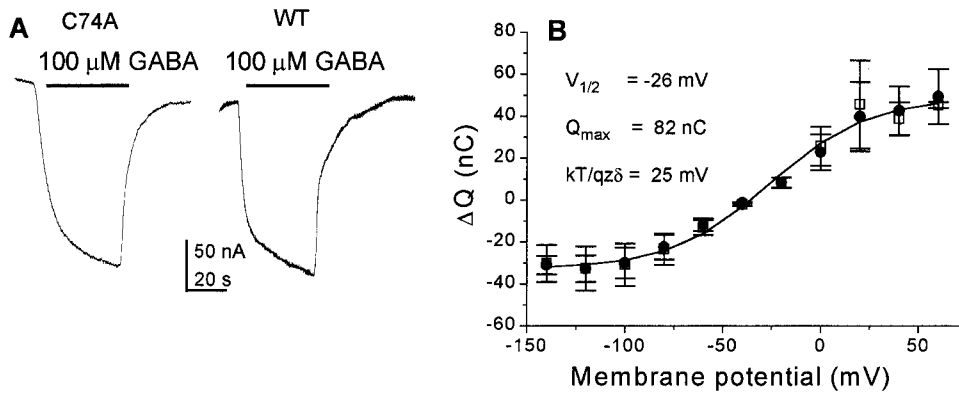
Figure 4. Comparison of WT-GAT1 and C74A electrophysiology after labeling with TMRM. Oocytes expressing WT-GAT1 and C74A-GAT1 were exposed to TMRM as described in **materials and methods**. (A) GABA-induced current was measured at a holding potential of −60 mV during perfusion of 100 mM GABA for a period of 4 s. The traces are typical of eight cells. (B) The charge movement (ΔQ) was calculated by integrating the transient current induced by a voltage jump from a holding potential of −40 mV to various test potentials, as shown in Fig. 5, middle. Each data point shows the average value from 40 cells for WT-GAT1 ($\square$) and 15 cells for C74A-GAT1 ($\blacksquare$). The error bars indicate SEM. The curve is a Boltzmann distribution with the indicated parameters.

equation (solid line). For both WT-GAT1 and C74A, $V_{1/2} = -26$ mV, $Q_{max} = 82$ nC, and $kT/qz\delta = 25$ mV. $V_{1/2}$ is the voltage at which charge movements are half completed, Q_{max} corresponds to the complete movement of charges between the membrane and the medium, z is the charge of the particle moving, δ is the fraction of the membrane field through which the charge moves, q is the elementary charge, and k and T have their usual meanings. The values for $V_{1/2}$, Q_{max}, and $kT/qz\delta$ are similar to previously reported values for WT-GAT1 (−27 mV, 80 nC, and 28 mV, respectively; Mager et al., 1993, 1996).

Interactions between TMRM and MTSET in Fluorescent Labeling

Yu et al. (1998) reported that exposure to another sulf-hydryl-reactive reagent, MTSET, caused nearly complete inhibition of WT-GAT1 transport-associated currents and charge movements. Since the C74A mutant was not sensitive to MTSET, the inhibitory effects of MTSET appear to be due exclusively to reaction with Cys74. Our fluorescence experiments did not employ MTSET-treated oocytes, but we compared the actions of MTSET and TMRM to determine whether TMRM labels GAT1 by reacting at the same cysteine residue(s) as MTSET. MTSET treatment blocked the uptake of [^{3}H]GABA by WT-GAT1 almost completely: from eight cells measured at 128 mM extracellular GABA, the uptake was 0.05 ± 0.01 pmol/oocyte per 20 min with MTSET treatment (Fig. 2). In contrast, TMRM labeling had no detectable effect on GABA uptake by WT-GAT1. The C74A transporter was much less sensitive to MTSET inhibition than WT-GAT1 (∼40% decrease, data not shown), in agreement with the electrophysiological data of Yu et al. (1998).

For the experiments presented in Table II, fluorescence was measured on oocytes reacted with TMRM and/or MTSET in all possible sequences. As expected from the data of Table I, the fluorescence intensity of TMRM was less in C74A-GAT1 than in WT-GAT1-expressing oocytes. Furthermore, the fluorescence intensity of TMRM-reacted WT-GAT1 oocytes was reduced by almost 50% when TMRM treatment was followed by MTSET reaction. For C74A-GAT1 oocytes, the percent reduction in the TMRM fluorescence intensity by MTSET was greater, 76%; however, the absolute value of the decrease in fluorescence signal was roughly equal (3–4 V) in the two cases. Furthermore, the fluorescence intensity for TMRM-labeled WT-GAT1 also exceeded that for TMRM-labeled C74A-GAT1 by 3–4 V. These results indicate (a) that the fluorescence signal in WT-GAT1 is caused by TMRM reaction with Cys74 and also with another residue, and (b) that TMRM fluorescence at this second residue is reduced by subsequent reaction with MTSET, via an unknown mechanism. Because the C74A transporter activity is not blocked by MTSET, it is clear that reaction of MTSET with cysteines other than Cys74 does not inhibit transporter function. Table II also presents results of the reverse series of exposures. After MTSET pretreatment, exposure to TMRM results in an increment of ∼4 V in fluorescence signals at both WT-GAT1 and C7A-GAT1. In the most straightforward interpretation of this result, MTSET alkylation prevents TMRM from labeling Cys74, but allows labeling at non-Cys74 sites.

We attempted to extend these observations in a set of electrophysiological measurements on oocytes before and after sequential TMRM and MTSET exposure. However, these dual exposures and repeated impalements rendered the oocytes so unhealthy that the results were inconclusive. Our experiments yield no decisive information about the fraction of Cys74 residues that are labeled by TMRM; we assume, but cannot prove, that this fraction is near unity. Nevertheless, the data do suggest that roughly half the steady state fluorescence signal arises from TMRM bound to Cys74. Furthermore, C74A-GAT1 provides a useful contrast to WT-GAT1 because C74A-GAT1 functions like WT-

	Fluorescence (V)			
	WT		C74A	
Control	0.2 ± 0.0	(*n* = 7)	0.2 ± 0.0	(*n* = 3)
TMRM*	8.2 ± 0.6	(*n* = 7)	5.0 ± 1.2	(*n* = 2)
TMRM followed by MTSET[‡]	4.9 ± 0.8	(*n* = 5)	1.2 ± 0.5	(*n* = 3)
MTSET[§]	0.2 ± 0.0	(*n* = 6)	0.2 ± 0.0	(*n* = 6)
MTSET followed by TMRM[‖]	4.3 ± 1.0	(*n* = 6)	4.8 ± 0.6	(*n* = 2)

*5 μM TMRM in ND96 solution was added to the oocyte chamber for 30 min at room temperature. [‡]After the TMRM treatment and washes, 3.75 mM MTSET was added to the oocyte chamber for 30 min. [§]3.75 mM MTSET in ND96 solution was added to the oocyte chamber for 30 min. [‖]After the MTSET treatment and washing, 5 μM TMRM in ND96 solution was added to the oocyte chamber for 30 min. Fluorescence intensity was measured as output from the PMT at a working voltage of 600 V, after 100× amplification.

GAT1, but is not labeled by TMRM at position Cys74. However, both MTSET and TMRM appear to react with one or more additional sites on GAT1. These observations provide the background for time-resolved measurements on TMRM-labeled GAT1 fluorescence during voltage jumps, reported in detail below.

Voltage Jumps Induce Fluorescence Changes in TMRM-labeled rGAT1

Fig. 5 presents a survey of simultaneous electrophysiological and optical signals recorded from oocytes in the apparatus described in Fig. 1. We used the voltage-jump protocol introduced by Mager et al. (1993) to elicit transient charge movements at GAT1 in the absence of GABA. As shown in Fig. 5 (top), the membrane potential was held at −40 mV, and then jumped to test potentials between +60 and −140 mV for a period of 350 ms. In uninjected oocytes reacted with TMRM (Fig. 5 A), there was no detectable change in fluorescence: the total variation was <0.1% over the voltage range studied. On the other hand, TMRM-labeled oocytes expressing WT-GAT1 (Fig. 5 B) displayed decreased fluorescence intensity during depolarizing jumps and increased fluorescence intensity during hyperpolarizing jumps. The total variation over the voltage range from +60 to −140 mV was ~0.8%. Evidently, these fluorescence signals are due to effects of the voltage jumps on the GAT1 molecules.

In the C74A mutant, there was a detectable but smaller fluorescence change, <0.4% over the range from +60 to −160 mV (Fig. 5 C). Again, depolarization decreased and hyperpolarization increased the fluorescence.

Fig. 6 shows the voltage and time dependence of the fluorescence signals in more detail. In Fig. 6, A and B, the fluorescence relaxations are fit to single exponen-

tials after suitable averaging and filtering (see materials and methods). For C74A-GAT1, the amplitude of the fluorescence change was approximately linear with voltage (Fig. 6 C). For example, the change over the 100-mV ranges from +60 to −40 mV and from −40 to −140 mV was 0.22 ± 0.01% and 0.20 ± 0.01%, respectively (mean ± SEM, *n* = 5 oocytes). In contrast, the fluorescence signals from WT-GAT1 were nonlinear with membrane potential: jumps to potentials more negative than −60 mV resulted in larger increases in fluorescence intensity than jumps to potentials more positive than −60 mV. When expressed as a percentage of background fluorescence, WT-GAT1 fluorescence relaxations at voltages more negative than −60 mV were 1.5- to 3-fold greater than C74A fluorescence relaxations; but because the absolute fluorescence intensity was 1.66-fold higher for oocytes expressing WT-GAT1 than for the C74A transporter, the absolute values of relaxations in WT-GAT1 oocytes were 2.5- and 4.5-fold larger than in C74A-GAT1 oocytes for jumps to −60 and −140 mV.

The time constant of the fluorescence relaxations showed much greater voltage dependence for WT-GAT1 than for the C74A mutant (Fig. 6 D). The average time constant of five C74A cells was between 75 and 103 ms for all voltages from +60 to −140 mV (Fig. 6 D), whereas the average time constant of five WT-GAT1 cells increased monotonically from 22 ± 1 ms at +60 mV to 151 ± 6 ms at −140 mV, a 6.5-fold change. An exponential fit of the voltage dependence of the WT-GAT1 time constants gave an e-fold change per 120 mV, but the value for C74A-GAT1 was at least 600 mV. Thus, although differences in fluorescence amplitude between WT-GAT1 and C74A-GAT1 are apparent only at membrane voltages from −60 to −140 mV (Fig. 6 C), the relaxation kinetics differ between WT-GAT1 and the C74A mutant over almost the entire voltage range accessible to experiment. In other words, the WT-GAT1 relaxation waveforms are not a simple sum of a Cys74-independent component plus an additional Cys74-specific component.

Tests for History Independence

In relaxation analysis, it is a fundamental concept that transition probabilities depend on the present value of parameters such as membrane potential, drug concentration, and temperature, but not on the history of these parameters. The apparently simple behavior of the relaxations allowed a test of this concept for the fluorescence signals (Figs. 7 and 8). The time constant of the fluorescence relaxation for WT-GAT1 did not depend strongly on the prepulse potential for steps to a constant test potential (−140 mV in the experiment of Fig. 7). The single-exponential time constant remained in the range from 122 to 155 ms as the prepulse voltage ranged from −100 to +60 mV (Fig. 7 C). The amplitude of the exponential component did of course depend on the prepulse
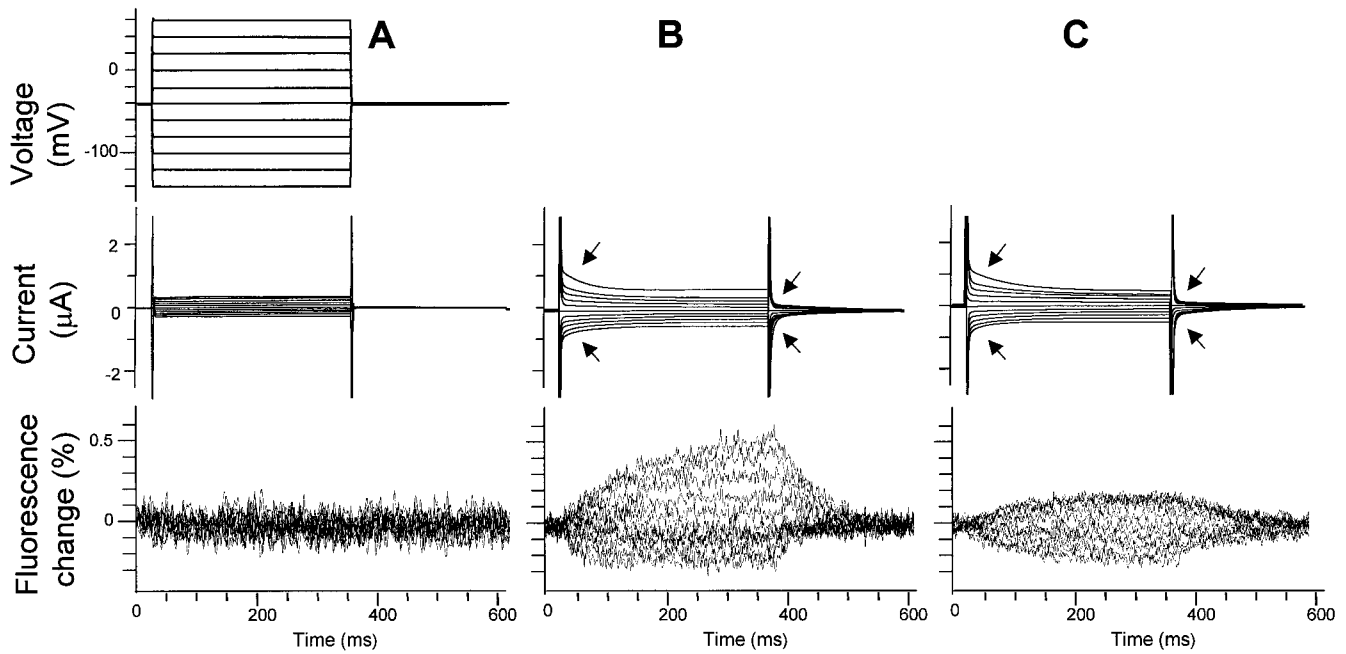
Figure 5. A survey of signals obtained with simultaneous recording of voltage-clamp current and fluorescence of TMRM-labeled GAT1 expressed in *Xenopus* oocytes. The voltage protocol is shown in A, top. The test potentials ranged from +60 to −140 mV in 20- mV increments. (Middle) The currents are shown. Arrows point to the transient currents that comprise the GAT1-specific charge movements. These transient currents far out last the endogenous capacitive currents of the oocyte membrane. The fluorescence signal is shown as the change of fluorescence intensity divided by the baseline fluorescence at the holding potential. Signals from an uninjected oocyte are shown in A. The current and fluorescence traces are the averaged signal from five cells for WT-GAT1 (B) and C74A-GAT1 (C).

potential, and decreased from 0.38% at a prepulse potential of +60 mV to 0.12% at a prepulse potential of −100 mV (Fig. 7 B). There was an additional component, with a time constant <10 ms, for the largest jumps (from voltages more positive than zero). This was a consistent finding among each of 40 cells tested.

This rapid component has not been examined systematically in our experiments.

In the complementary experiment, we studied the kinetics of the fluorescence decrease due to a voltage jump from a constant hyperpolarizing voltage (−140 mV) to varying depolarized levels (between −60 and
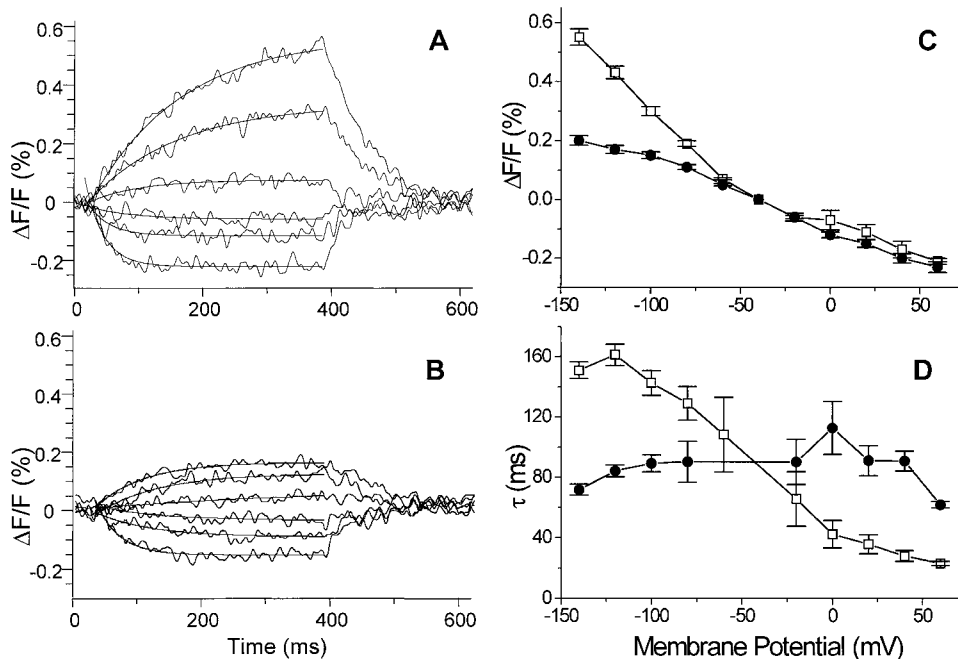

Figure 6. Analysis of the fluorescence relaxations. The fluorescence from Fig. 5 is replotted for odd-numbered traces (test potentials between +60 and −140 mV in 40-mV increments). The fluorescence relaxations for WT-GAT1 (A) and C74A–GAT1 (B) were fit to single-exponential processes, which are superimposed on the traces. The amplitude ($\Delta F/F$) and time constant t from the fits are plotted as functions of test potential in C and D for WT-GAT1 (□) and C74A-GAT1 (●). Error bars indicate standard error of the fits using CLAMPFIT 8.
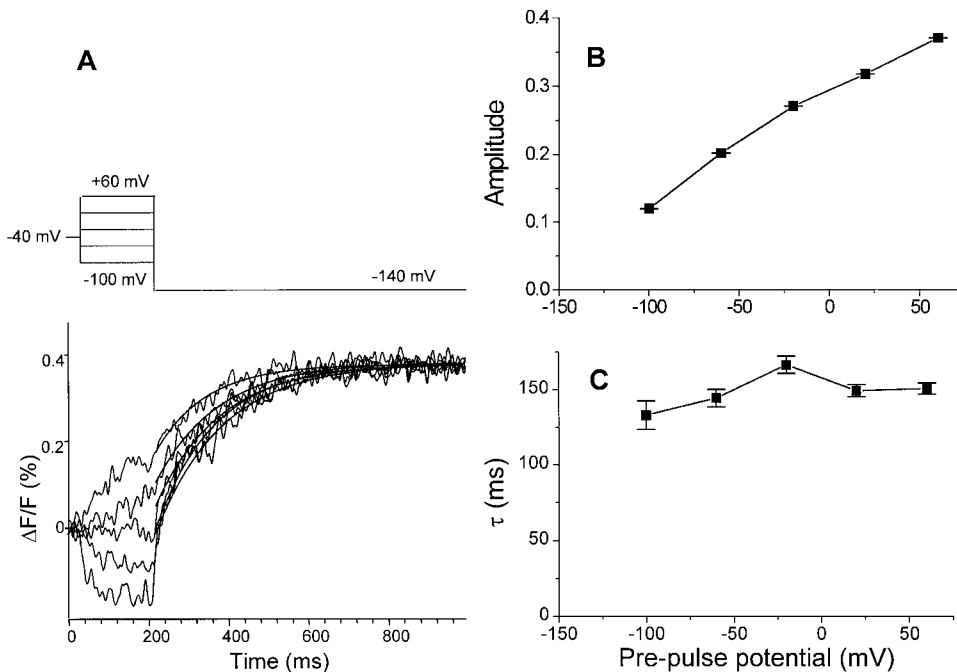
497   Li et al.

Figure 7. Tests for history dependence: effect of prepulse potential on the fluorescence relaxation. (A) Typical fluorescence traces from one WT-GAT1 cell. (Top) The voltage protocol is shown. The results from single-exponential fits to the rising phase of the fluorescence are superimposed on the traces. The amplitude (B) and time constant (C) from the fit are plotted as function of prepulse potential. Error bars indicate standard error of the fit using CLAMPFIT 8.

+60 mV). The results are shown in Fig. 8. Unlike the previous experiment, the time constant of the fluorescence decrease was dramatically affected by the membrane potential of the test pulse: the time constant increased from 30 ± 1 ms at $+60$ mV to 100 ± 3 ms at -60 mV, a threefold increase (Fig. 8 C). At each voltage, these time constants are similar to the values measured for jumps from a prepulse potential of -40 mV (Fig. 6). Fluorescence relaxations, therefore, appear to conform to the concept that the relaxation rates depend on the present value of the membrane potential rather than on its history.

Comparison of Fluorescence and Charge Movement

As noted above, voltage jumps evoke transient capacitive currents at WT-GAT1. The voltage dependence and kinetics of these charge movements have been analyzed in detail previously (Mager et al., 1993, 1996; Lu et al., 1996; Hilgemann and Lu, 1999; Lu and Hilgemann, 1999b), and in this study we found that the TMRM labeling procedure does not affect these transient currents (Fig. 4 B). The transient currents are absent in uninjected oocytes (Fig. 5). This charge movement represents Na^+ binding with the transporter and/or the conformational change induced by Na^+ binding (Mager et al., 1993). The time constant of the charge movement is tens to hundreds of milliseconds, similar to that of the fluorescence change.

Fig. 9 compares the voltage dependence and kinetics of the capacitive charge movements with those of the fluorescence relaxations. Data from five cells were averaged, and the amplitudes of the fluorescence change

and charge movement were plotted as a function of membrane voltage. As seen in the figure, the plot of fluorescence lies to left of the plot of charge movement by at least 50 mV (Fig. 9 A). Furthermore, the fluorescence shows no sign of saturation with hyperpolarization, so that the midpoint of the fluorescence–voltage relation cannot be determined. Although we know that the midpoint of the charge–voltage relation is approximately -26 mV (Fig. 4), we know only that the midpoint of the fluorescence–voltage relation is more negative than approximately -75 mV. The actual difference between charge and fluorescence is thus at least 50 mV on the voltage axis.

Despite the similar range of time constants for the charge movements and the fluorescence signals, they differ significantly in value at almost every voltage tested between $+60$ and -140 mV (Fig. 9 B). Furthermore, the time constants characterizing the fluorescence change and charge movement have distinct dependences on membrane potential (Fig. 9 B). While the time constant of the fluorescence change increases monotonically with hyperpolarizing voltages (with perhaps a hint of saturation at the highest negative potentials), the time constant of charge movement shows a maximum at -40 mV (Fig. 9 B; see also Mager et al., 1996).

An Alternative Subtraction Procedure Confirms the Distinct Voltage Dependences of Charge Movement and Fluorescence

Because the fluorescence signals are small, we sought additional tests of the conclusion that the fluorescence signal occurs at membrane potentials more hyperpolarized than the charge movement. The amplitude of the
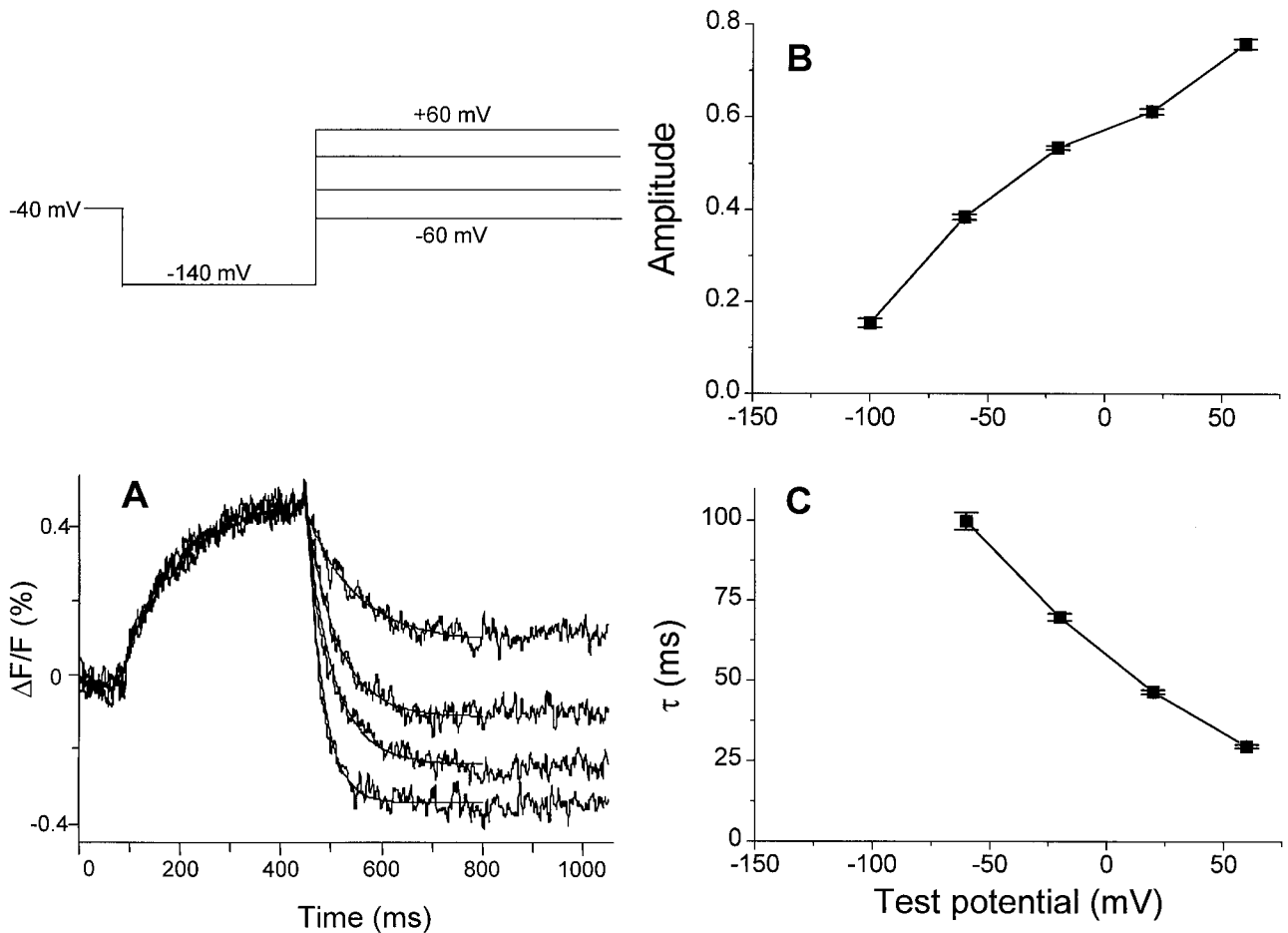
Figure 8. Tests for history dependence: effect of test potential on the fluorescence relaxation. (A) Typical traces from the average of 100 sweeps. (Top) The voltage protocol is shown. The results from single-exponential fits to the falling phase of the fluorescence are superimposed on the traces. The amplitude (B) and time constant (C) are plotted as functions of the test potential. Error bars indicate standard error of the fit using CLAMPFIT 8.

fluorescence relaxations for C74A, expressed as $\Delta F/F$, equals that of WT-GAT1 for most of the voltage range (Fig. 6). As discussed above, WT-GAT1 fluorescence waveforms cannot be expressed simply as a sum of Cys74-dependent and -independent terms. Nevertheless, we subtracted the fluorescence signal of C74A from that of WT-GAT1 (both expressed as $\Delta F/F$) to ap-

proximate a site-specific fluorescence signal from residue Cys74. The resulting waveforms are shown in Fig. 10 A. Using this analysis, fluorescence relaxations due to TMRM labeling at C74 appear to occur only at hyperpolarized voltages (more negative than −40 mV). The fluorescence increased with hyperpolarizing membrane potentials; there were no signs of saturation at
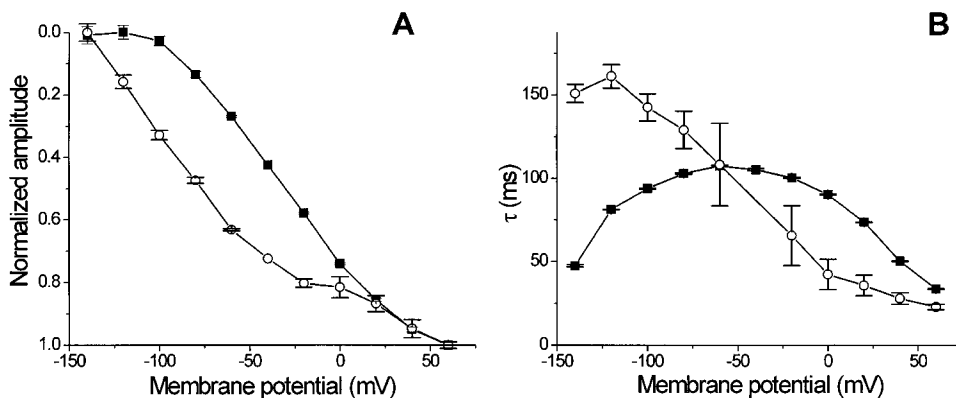

Figure 9. Comparison of the voltage dependence of the fluorescence relaxations and the charge movements. The normalized amplitude (A) and time constant (B) from single-exponential fits of the fluorescence change (○) and charge movement (■). The charge movement data are those plotted in Fig. 4 B, inverted to simplify the comparison to fluorescence. Error bars indicate standard error of the fit using CLAMPFIT 8.

the most negative membrane potential tested, -140 mV (Fig. 10 B). The fluorescence relaxation fit well to a single exponential process with time constant ranging from 75 to 150 ms at potentials from -40 to -140 mV (Fig. 10 C). These observations on voltage dependence and kinetics agree well with the characteristics of the unsubtracted traces (Figs. 6–9). Thus, the details of the signal analyses do not strongly affect the conclusion that distinct voltage dependences characterize the fluorescence change and the charge movements.

Effect of Substrates

The effect of GAT1 substrates, GABA, Na^+ and Cl^- on the electrophysiological properties of GAT1 was studied previously in our laboratory (Mager et al., 1993, 1996). The results show that GABA induces transport-associated currents that depend on $[Na^+]$, $[Cl^-]$, $[GABA]$, and membrane potential. The transport-associated current discharges the capacitance of GAT1. In the absence of GABA, $[Na^+]$ and $[Cl^-]$ influence these capacitive charge movements as follows. Reduced $[Na^+]$ and $[Cl^-]$ shift the charge movement–membrane potential curve to more hyperpolarized potentials (Mager et al., 1993, 1996). The shift is more dramatic for Na^+ removal than for Cl^- removal. In particular, for a hyperpolarizing voltage jump from -40 to -140 mV, the charge movement is not altered by various concentrations of Cl^-, but is blocked by zero concentration of Na^+ (Mager et al., 1993, 1996). All these characteristics of transport-associated currents and charge movements were noted, though not studied quantitatively, in the

electrophysiological recordings that accompanied each fluorescence experiment in the present study.

The effects of changing these substrates on the fluorescence signal of GAT1 are shown in Fig. 11. The top panels show exemplar fluorescence traces for the voltage-jump relaxations from -40 to -140 mV; The bottom panels present the effects of GAT1 substrates on the fluorescence amplitude averaged across several complete voltage-jump experiments, like those of Fig. 5, at test potentials in the range $+40$ to -140 mV. GABA produced virtually no change in the amplitude of the fluorescence relaxations (although the simultaneous voltage-clamp measurements revealed that the charge movements were shunted and became GABA-induced currents as expected).

Cl^- substitution with gluconate modestly decreased the amplitude of fluorescence relaxations, by 10–50%, at voltages more negative than -60 mV (Fig. 11, B1 and B2). If the effect of Cl^- replacement by gluconate is treated as a shift in the fluorescence–voltage relation, the shift amounts to ~15 mV in the negative direction. This is considerably less than the ~44-mV negative shift reported for the same ionic replacement in charge movement experiments (Mager et al., 1993). Kinetic analyses on the effects of substrate substitution on the fluorescence signal (summarized in Table III) reveal that Cl^- substitution with gluconate introduced a new slower process with time constant of 308 ± 20 ms ($n = 4$) to the fluorescence increase. This time constant should be considered an estimate, because the relaxation did not reach steady state during the 500-ms test
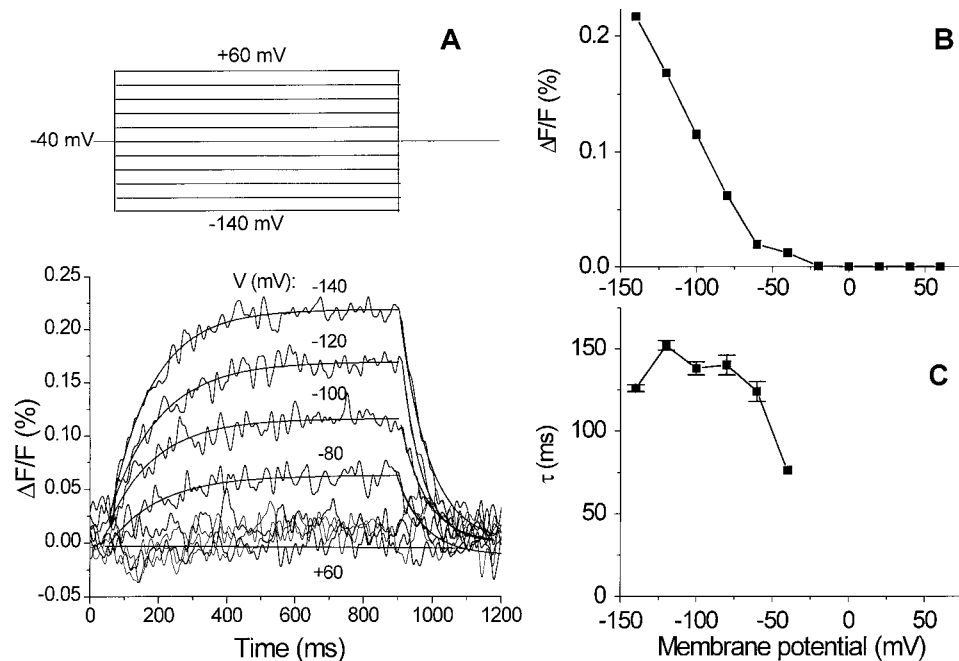

Figure 10. An alternative analysis of voltage dependence. (A) The fluorescence signal from an oocyte expressing TMRM-C74A-GAT1 was subtracted from the signal from another cell expressing TMRM-WT-GAT1. The curves are single-exponential fits to the fluorescence relaxations. (Top) The membrane potential was held at -40 mV and stepped to various test potentials. (B) The amplitudes of the fluorescence change were plotted as a function of membrane potential. (C) The time constants for the rising (-80, -100, -120, -140) or falling (-40 mV) phase of the fluorescence are plotted versus the membrane potential. Error bars indicate standard error of the fit.
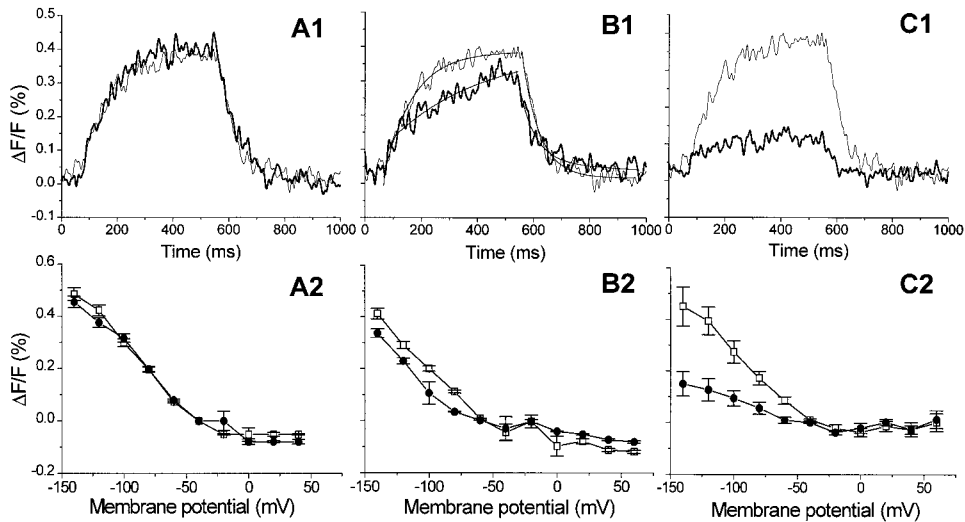
Figure 11. Effect of GAT1 substrates GABA, Cl^- and Na^+ on the fluorescence change. (Top) Typical fluorescence traces from one cell recorded in solutions containing various combinations of GABA, Cl^-, and Na^+. The membrane potential was held at -40 mV, stepped to a test potential of -140 mV for 550 ms, and then stepped back to -40 mV. (Bottom) Voltage dependence of the amplitude of the fluorescence change for the averaged data from five oocytes, $\pm$SEM. The recording solution for the control traces was ND96, as described in materials and methods. (A) Effect of GABA. The fluorescence was recorded in the absence (light traces) and presence (heavy traces) of 100 mM GABA. (B) Effect of Cl^-. The fluorescence was recorded in the presence (light traces) and absence (heavy traces) of 96 mM Cl^-. Cl^- was substituted with gluconate. (C) Effect of Na^+. The fluorescence was recorded in the presence (light traces) and absence (heavy traces) of 96 mM Na^+. Na^+ was substituted with NMDG.

pulse. Nevertheless, the overall effect of Cl^- substitution was clearly to slow the time course of the fluorescence increase with only a modest change in amplitude (the amplitude of the fluorescence change was $0.41 \pm 0.01\%$ in the presence of Na^+ and Cl^- and $0.37 \pm 0.01\%$ in the absence of Cl^-).

On the other hand, Na^+ substitution with NMDG blocked most of the fluorescence signal. Of >20 cells studied, for the jump from -40 to -140 mV, the amplitude of the fluorescence change was decreased by ninefold in the absence of Na^+, and there were similar reductions at all voltages more negative than -60 mV. The remaining relaxation had a time constant of 32 ± 4 ms ($n = 4$). Table III also shows that the time course of the fluorescence decrease for the voltage jump from -140 to -40 mV was not significantly affected by Cl^- but was affected by Na^+. In the presence of both Na^+ and Cl^-, the fluorescence decrease is a single exponential process with time constant of 59 ± 1 ms ($n = 4$). In the absence of Cl^- (substitution by gluconate) and presence of Na^+, the time constant of the fluorescence decrease was 56 ± 4 ms ($n = 4$). The time course of the fluorescence decrease was dramatically affected by the absence of Na^+: the time constant decreased to 9 ± 1 ms ($n = 4$).

Na⁺ Concentration Dependence of the Fluorescence Relaxations

The Na^+ dependence of the fluorescence was further studied by varying the Na^+ concentration in the extracellular medium. The results are shown in Fig. 12. To study the Na^+-dependent fluorescence signal, the residual small fluorescence that is Na^+ independent was subtracted from each trace. Upon voltage jump from -40 to -140 mV, the fluorescence increased in a single-exponential process (Fig. 12 A). Both the ampli-

tude and the time constant of the fluorescence change depended on the Na^+ concentration. Because there was no apparent saturation with Na^+ concentration, the plot of fluorescence amplitude–Na^+ concentration was fit to a power law (as though it were the foot of a Hill function). The exponent was 1.8 (Fig. 12 B), which is consistent with the observation from previous studies that two Na^+ interact with GAT1 (Mager et al., 1993). The plot of the rate constant of the fluorescence increase upon hyperpolarizing voltage jump, $1/\tau_{-140 \text{ mV}}$, vs. $[Na^+]$ was fit to a straight line, resulting in a slope of $64 \text{ M}^{-1}\text{s}^{-1}$ (Fig. 12 C). Although complete removal of Na^+ did dramatically accelerate the fluorescence decrease for the jump from -140 to -40 mV (Table III), there was no systematic effect of Na^+ concentration in the range from 48 to 96 mM; the rate constant, $1/\tau_{-40 \text{ mV}}$, varied between 13 and 18 s^{-1} (Fig. 12 D).

TABLE III

*Parameters for the Rising and Falling Phases of TMRM-WT-GAT1 Fluorescence**

		In ND96	In Gluconate	In NMDG
A_1 (%)	Rising phase	0.39 ± 0.03	0.13 ± 0.01	0.14 ± 0.02
	Falling phase	0.47 ± 0.02	0.41 ± 0.02	0.12 ± 0.01
τ_1 (ms)	Rising phase	90 ± 1	64 ± 6	32 ± 4
	Falling phase	59 ± 1	56 ± 4	9 ± 1
A_2 (%)	Rising phase		0.26 ± 0.01	
τ_2 (ms)	Rising phase		308 ± 20	

*Fluorescence signals (Fig. 13) were measured from the TMRM-labeled WT-GAT1 upon voltage jump from -40 to -140 mV (rising phase) and back to -40 mV (falling phase), and fit to the equation, $F(t) = \Sigma A_i \exp(-t/\tau_i) + C$. Data are presented as mean $\pm$ SEM ($n = 4$).
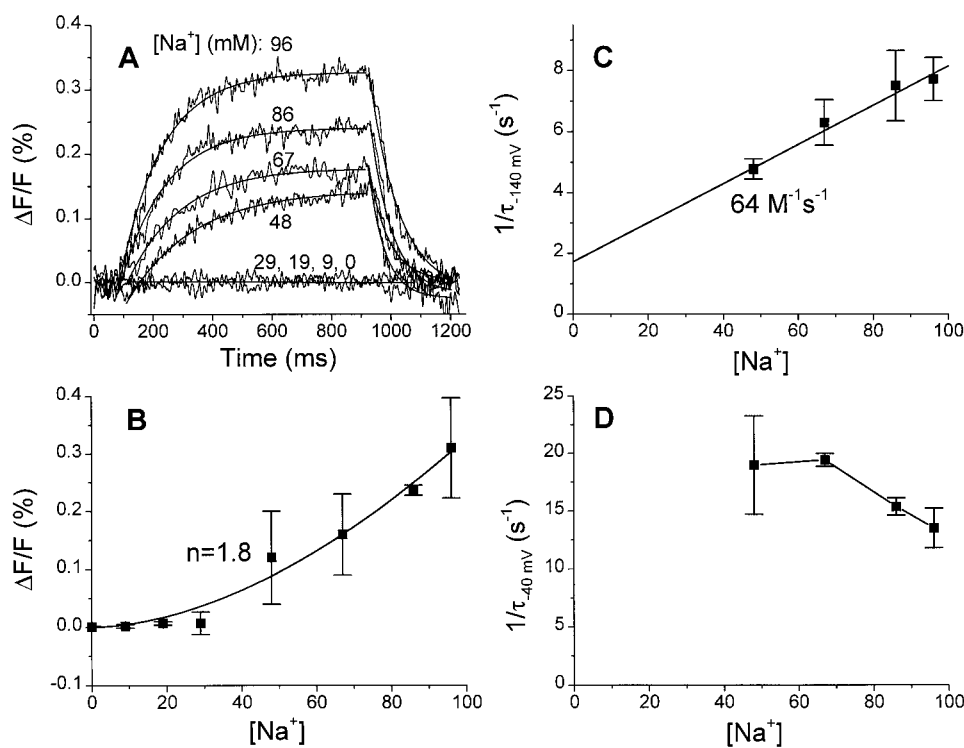
Figure 12. Effect of extracellular Na^+ concentration on the fluorescence signal. (A) The fluorescence traces are the averaged traces from four cells. The curves show single-exponential fits to the traces. The membrane potential was held at -40 mV, stepped to a test potential of -140 mV for 800 ms, and then jumped back to the -40-mV holding potential. The recording solution was ND96, as described in the materials and methods, in which Na^+ was substituted with various concentrations of NMDG. The residual small fluorescence at 0 $[Na^+]$ ($\sim0.05\%$) was subtracted from each trace to show the Na^+-dependent fluorescence signal. (B) The amplitude of the fluorescence change, plotted as a function of the Na^+ concentration. The curve represents the equation $\Delta F/F = a [Na^+]^{1.8}$. (C) The rate constants of single-exponential fits to the rising phase of the fluorescence relaxation are plotted as a function of Na^+ concentration. The linear fit is superimposed on the data, and the slope equals 64 $M^{-1}s^{-1}$. (D) Rate constants from single-exponential fits to the falling phase of the fluorescence for the jump from -140 to -40 mV are plotted as function of Na^+ concentration. The lines connect the data points. For all panels, data points are mean $\pm$ SEM ($n = 4$ cells).

Effect of a Transport Inhibitor

The GAT1 inhibitor, NO-711 (Fig. 13 A), was studied for its effect on the fluorescence and charge movement of GAT1. NO-711 blocked the charge movements of GAT1 during voltage jumps, as found in earlier studies (Mager et al., 1993, 1994). Also, in more than 20 cells studied, NO-711 decreased the fluorescence relaxations (Fig. 13 B). The effect of NO-711 on the fluorescence amplitude was also studied at various test potentials, and the results are shown in Fig. 13 C. NO-711 decreased the fluorescence by $\sim80\%$ at hyperpolarizing membrane voltages.

The W68L Mutation Shows Fluorescence Relaxations Only at High Positive Potentials

We also labeled oocytes expressing the GAT1-W68L mutation (Kleinberger-Doron and Kanner, 1994; Mager et al., 1996). The fluorescence labeling intensity from 6 W68L oocytes was 105% that of 10 WT oocytes in the same batch; this small difference is not significant. Yet in each of two oocyte batches, the fluorescence relaxations from GAT1-W68L oocytes were quite small over most of the voltage range: detectable signals were noted only at the most positive membrane potentials and were only $\sim0.2\%$ in amplitude (Fig. 14). The only relaxations large enough for kinetic analysis were evoked by the jump from –40 mV to +60 mV; the time

constant was 133 ± 14 ms, greater than that either for the WT or C74A transporter and 2-3 times larger than the time constant for W68L charge movements under similar conditions (Mager et al., 1996). We emphasize that WT-GAT1 yielded normal fluorescence relaxations signals in oocytes from the same batches.

That W68L-GAT1 produces detectable fluorescence relaxations under jumps to high positive potentials fits well with the idea that the fluorescence relaxations monitor transitions of active transporters. In previous studies, W68L-GAT1 showed GABA transport and transport-associated currents <10% those of WT-GAT1 (Kleinberger-Doron and Kanner, 1994; Mager et al., 1996). Furthermore, the relation between charge movements and membrane potential for W68L is shifted toward the right by ~130 mV compared with the WT transporter. Only small charge movements are observed, and only for jumps to membrane potentials more positive than $+40$ mV (Mager et al., 1996). Fig. 14 (top) confirms that slow capacitive transients, indicative of W68L-GAT1 charge movements, occur only at the high positive potentials where the fluorescence relaxations are also observed.

DISCUSSION

These experiments introduce simultaneous measurements on electrophysiology and fluorescence for the
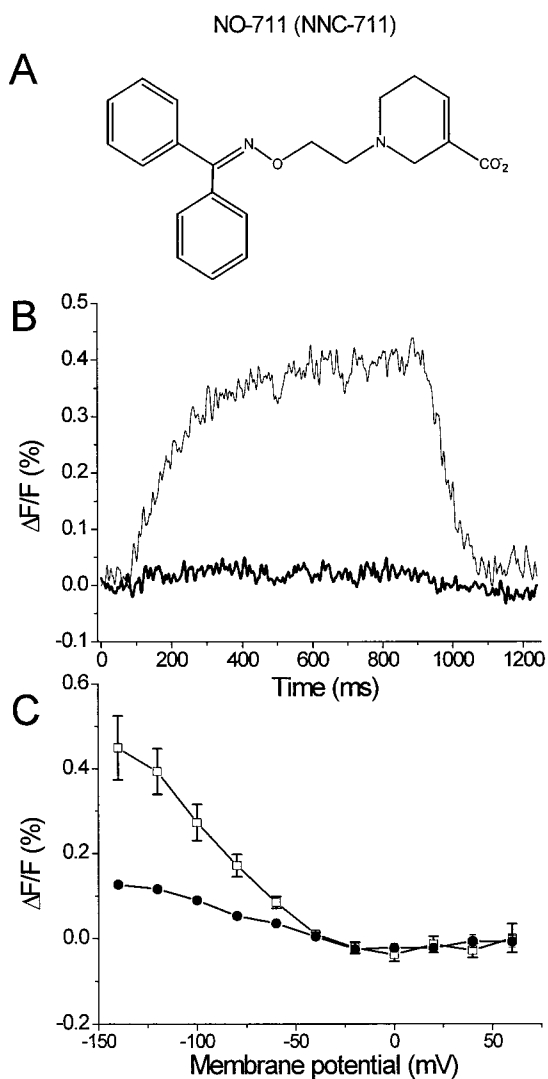
NO-711 (NNC-711)

A

B

C

Figure 13. Effect of GAT1 inhibitor, NO-711, on the fluorescence relaxations. (A) The structure of the compound. (B) Typical traces from one cell in the absence (light trace) and presence (heavy trace) of 3 mM NO-711. The voltage was held at -40 mV and stepped to a test potential of -140 mV. The cells were incubated in ND96 containing NO-711 for at least 5 min before recording. (C) Voltage dependence of the amplitude of the fluorescence relaxation, recorded in the absence ($\square$) and presence ($\bullet$) of 3 mM NO-711 (B2). Data points are mean $\pm$ SEM ($n = 6$ cells).

study of a neurotransmitter transporter. The data show that specific fluorescence signals are obtained when the GABA transporter GAT1 is subjected to jumps in membrane potential. Proof that the signals arise directly from functional GAT1 comes from several facts. (a) The signals depend absolutely on GAT1 expression. (b) The point mutant C74A produces distinct signals. (c) The poorly functional W68L transporter displays WT levels of steady state fluorescent labeling, but only small relaxations and only under the same restricted conditions that also produce charge movements. The
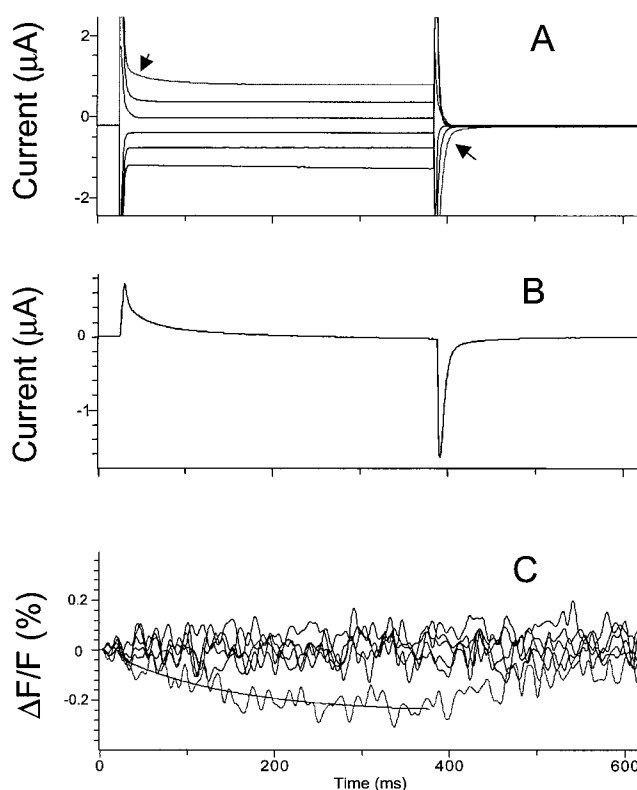
A

B

C

Figure 14. The W68L-GAT1 mutant shows signals only at high positive potentials. The membrane potential was held at -40 mV and jumped to test potentials between $+60$ and -140 mV in 20-mV increments. The traces show the signals for the jumps to $+60$, $+20$, -20, -60, -100, and -140 mV, as in Fig. 6. Signals for six oocytes have been averaged. (A) Voltage-clamp currents. The arrows point to the trace for the jump to $+60$ mV; this is the only jump that evoked measurable charge movements. (B) Traces for the jumps from -40 to -140 mV and from -40 to $+60$ mV have been added to isolate the voltage-dependent capacitive currents for the jumps to and from $+60$ mV while subtracting the passive resistive and capacitive currents. (C) The fluorescence signals; only the jump to $+60$ mV evoked fluorescence relaxations large enough (approximately -0.2%) for kinetic analysis. The jumps to $+40$ mV are not shown, but also gave barely perceptible charge movements and fluorescence relaxations.

results for W68L-GAT1 would be significant even if there were no fluorescence signals at all; the argument does not depend on the small signals for jumps to $+40$ and $+60$ mV, but does depend on the normal level of fluorescence labeling combined with the absence of most fluorescence relaxations. (d) The GABA uptake inhibitor NO-711 blocks the fluorescence relaxations. These observations eliminate a number of admittedly unlikely artifacts arising from (a) nonspecific effects of membrane protein expression or (b) accessory proteins that might be brought to the membrane by GAT1.

The data also show that part of the fluorescence signal arises at Cys74, a residue thought to lie in the first extracellular loop (Yu et al., 1998). In the C74A mutant subjected to similar labeling procedures, the trans-

porter functions nearly normally (Fig. 4), yet the steady state fluorescence is reduced by ~40% (Table I) and the voltage-dependent fractional change in fluorescence is reduced by at least twofold at voltages more negative than −80 mV (Figs. 5 and 6).

There are non-Cys74 signals as well; these appear to depend linearly on membrane potential. However, the fact that we measure single but different time constants in the presence and absence of Cys74 suggests that the signals are not a simple sum of Cys74 and non-Cys74 components, vitiating a clear view of possible interactions among fluorescent labels. Interpretation of the non-Cys74 signals is also complicated by four additional observations about effects of sulfhydryl reagents. (a) In the present experiments, TMRM labeling could occur at non-Cys74 sites despite previous reaction with MTSET, but could also be reversed by subsequent exposure to MTSET (Table II). (b) Reactivity at Cys residues other than Cys74 may depend on the functional state of the transporter (Golovanevsky and Kanner, 1999), and there are complex interactions involving the analogous position in SERT, C109 (Stephan et al., 1999). (c) Rather severe exposure to MTSET is required to alkylate Cys74 (Yu et al., 1998); concentrations of 1.5 mM (vs. 3.75 mM used in the present experiments) and incubations of 5 min (vs. 30 min in the present experiments) produced no blockade (Bennett and Kanner, 1997). (d) Both TMRM and MTSET may react with other functional groups (Means and Feeney, 1971; Kluger and Tsui, 1980).

The fluorescence signals are small, limiting our ability to resolve their detailed amplitude and time course under varying conditions. The largest change in fluorescence that we observed, corresponding to voltage jumps between +60 and −140 mV, amounted to 0.8%. Our apparatus works well, as judged by the robust signals (31%) obtained with a similarly labeled K^+ channel (Mannuzzu et al., 1996). Furthermore, these small signals occur despite an impressive expression level: the 80 nC of charge movement corresponds to a transporter density of ~20,000/μm^2 (Mager et al., 1993). Despite the small signals, we introduce history independence as a test for well-behaved conformational transitions, and we show that quantitative comparisons of voltage dependence can be made between fluorescence and charge movements.

In addition to the challenges posed by temporal analysis of the relaxations, other uncertainties are raised in evaluating the steady state fluorescence intensities. Previous studies show that changing the concentration of inhibitors, of Na^+, or of Cl^- at constant voltage produces charge movements associated with ion binding to GAT1 (Mager et al., 1993, 1996). Changes in the concentrations of these agents also affect our fluorescence relaxations and therefore might also change steady state fluorescence under our baseline conditions (usually −40

mV). However, these variations would be expected to lie within the same amplitude range as the voltage-jump relaxations, <1%. Signals this small, occurring over several seconds, would not be distinguishable from drifts caused by bleaching and oocyte motions. Although the figures present aligned baselines, it is likely that exposure to inhibitors or to varying substrate concentrations has changed the baseline fluorescence. We think it likely that the W68L transporter is actually fixed at a steady state fluorescence level similar to that attained by the WT transporter only at large negative potentials, because previous studies suggest that the W68L transporter is blocked at a point in the transport cycle after the binding of Na^+ and before that of GABA (Mager et al., 1996). Similar comments apply to the fluorescence in the presence of NO-711 (Mager et al., 1996).

Despite these limitations, the experiments clearly show that the fluorescence signals differ in important ways from the previously known signals, primarily electrophysiological, associated with GAT1 function. The dependence on membrane potential (Figs. 9 and 10), GABA (Fig. 11), Cl^- concentration (Fig. 11), and Na^+ concentration (Fig. 12) all differ markedly from the characteristics of the transport-associated currents and transient charge movements described in previous studies (Mager et al., 1993, 1996; Lu et al., 1996; Hilgemann and Lu, 1999; Lu and Hilgemann, 1999b). The kinetics of the major fluorescence signal (time constant of 30–150 ms) are in the range of those expected from a rate-limiting process in the transport cycle, but detailed analysis shows that the kinetics do not match the well-studied process associated with Na^+ binding to the transporter. These observations differ from the impressive correlations with electrophysiology obtained in fluorescence studies on voltage-gated channels (Mannuzzu et al., 1996; Siegel and Isacoff, 1997) or, more relevant, on the Na^+-glucose transporter SGLT1 labeled at position 457 (Loo et al., 1998).

Nature of the Voltage-induced Fluorescence Signal

The effects of jumping the membrane voltage on GAT1 could have one or more of three physical bases. (a) Membrane potential changes the electrochemical gradient of the charged GAT1 substrates, Na^+ and Cl^-. Under most of our conditions, a hyperpolarizing voltage jump increases the electrochemical driving force for Na^+, thus possibly changing the balance of transporters among intermediate states in the transport cycle. (b) A jump in the membrane electrical field could change in the energy barrier for some conformational changes during GAT1 function. These conformational changes could involve entire domains of the protein, or individual side chains. (c) In a related mechanism, the covalently attached fluorophore itself, which has a substantial dipole moment, could move in the field.

Changes in fluorescence of reporter groups are thought to arise from changes either in the polarity of the immediate environment and/or in quenching by discrete neighboring moieties. Any of the mechanisms described above could involve such changes. In addition, one should consider (d) altered quenching by ions bound nearby. We also cannot rule out changes in quenching due to interactions between neighboring fluorophores, although modern studies have shown no evidence that transporters similar to GAT1 exist as multimers (Eskandari et al., 1998).

The fact that the fluorescence signal from WT-GAT1 is a nonlinear function of voltage argues against hypotheses c and d, which would be expected to produce effects that are linear, at least to first order, with the membrane field. A related observation, that W68L-GAT1 displays fluorescence relaxations only at the high positive potentials that also permit conformational changes (Fig. 14) (Mager et al., 1996), supports the hypothesis that the fluorescence changes do not originate from nonspecific movement of charged groups within the electrical field in response to voltage jumps. Therefore, we conclude that the fluorescence relaxation observed in GAT1 corresponds to a conformational change of GAT1 induced either by increased electrochemical driving force of Na^+ and/or by a decreased energy barrier between two conformational states of GAT1.[2] In fact, these two mechanisms may be indistinguishable at the level of the finest details of the transport mechanism (Su et al., 1996; Lester et al., 1996).

Nature of the Fluorescent State

A conformational change produces the fluorescence signal. Conformational changes form the basis of kinetic-state models for GAT1 function studied by Hilgemann and Lu (1999). Their favored model is shown in Fig. 15. Dr. Hilgemann kindly spent some effort at investigating states in this model that might parallel our signals, but was unable to correlate the fluorescence signals shown here with a kinetic state in their model. We suggest that the fluorescence relaxations observed with TMRM-labeled GAT1 accompany transitions to and from a novel intermediate state that was not detectable in the experiments of Hilgemann and Lu (Fig. 15). Hilgemann concluded that the transition from E^*_{out} to E_{out} is voltage dependent, occludes a Na^+ onto the transporter, and constitutes the major rate-limiting step

in the transport cycle (Hilgemann and Lu, 1999). It is therefore not surprising that an additional detection technique—fluorescence labeling in this case—has produced evidence for the existence of an additional step during this complex E^*_{out} to E_{out} transition. Because the novel state lies between the two states, E^*_{out} and E_{out}, we term the new state E^*_{out}-*fluo*. Our measurements do not accurately reflect the steady state fluorescence, but do track changes from this baseline level; therefore, the measurements are expected to reflect primarily the relative levels of E^*_{out}-*fluo* and the two adjacent states, E^*_{out} and E_{out}. Fig. 15 explains how the scheme accounts for the data in the present study: membrane potential, Na^+, NO-711, and the W68L mutation all affect the fluorescence relaxations strongly, while Cl^- and GABA affect the relaxations more weakly, if at all.

We were initially surprised that GABA does not strongly affect the relaxations. However, we emphasize that most transporters are thought to reside in the states that include E^*_{out}, E^*_{out}-*fluo*, and E_{out}, both in the presence and absence of GABA (Lester et al., 1996; Hilgemann and Lu, 1999). This point accounts for the relative lack of GABA effects on the relaxations.

Our study thus supports kinetic models in which multiple conformational changes occur during neurotransmitter transporter function, and our data suggest that one such conformational change comprises part of the transition previously thought to limit the rate of transport (Mager et al., 1993, 1996; Hilgemann and Lu, 1999). Because ion-coupled transport can be simulated in the absence of conformational changes (Su et al., 1996), this is a noteworthy observation. The magnitude of the fluorescence changes that we observe is very small; therefore, we cannot yet make quantitative statements about the newly identified intermediate state. However, much of our data suggests that E^*_{out}-*fluo* is poorly populated under the conditions of all our manipulations. The fluorescence relaxations show no sign of saturation with hyperpolarizing voltage even at the most negative potentials studied (-140 mV); thus, at most half the transporter population is in the fluorescent state. The signal also shows no sign of saturation with Na^+ concentration even at the highest levels studied (96 mM); this implies a similar factor of 50%. We shall assume that these factors are multiplicative, implying that even our largest signals correspond to an E^*_{out}-*fluo* occupancy of at most 25%. Perhaps only a few percent of the transporters are in E^*_{out}-*fluo*. This hypothesis also partially explains (a) the small size of the signal and (b) the fact that E^*_{out}-*fluo* escaped detection in the experiments of Lu and Hilgemann (1999a,b).

Relationship to Other Work

We believe that we have detected a conformational change in GAT1 near Cys74. The importance of this re-

---

[2]On the other hand, the linear voltage dependence of the fluorescence signal from the C74A mutant would be explained by contributions from any or all of these four mechanisms. However, W68L-GAT1 both undergoes conformational changes and displays fluorescence relaxations, only at positive potentials, suggesting that even the C74A signals arise from specific conformational changes. We have little data to suggest the nature of the conformational changes monitored by the C74A signals and will not consider them further.
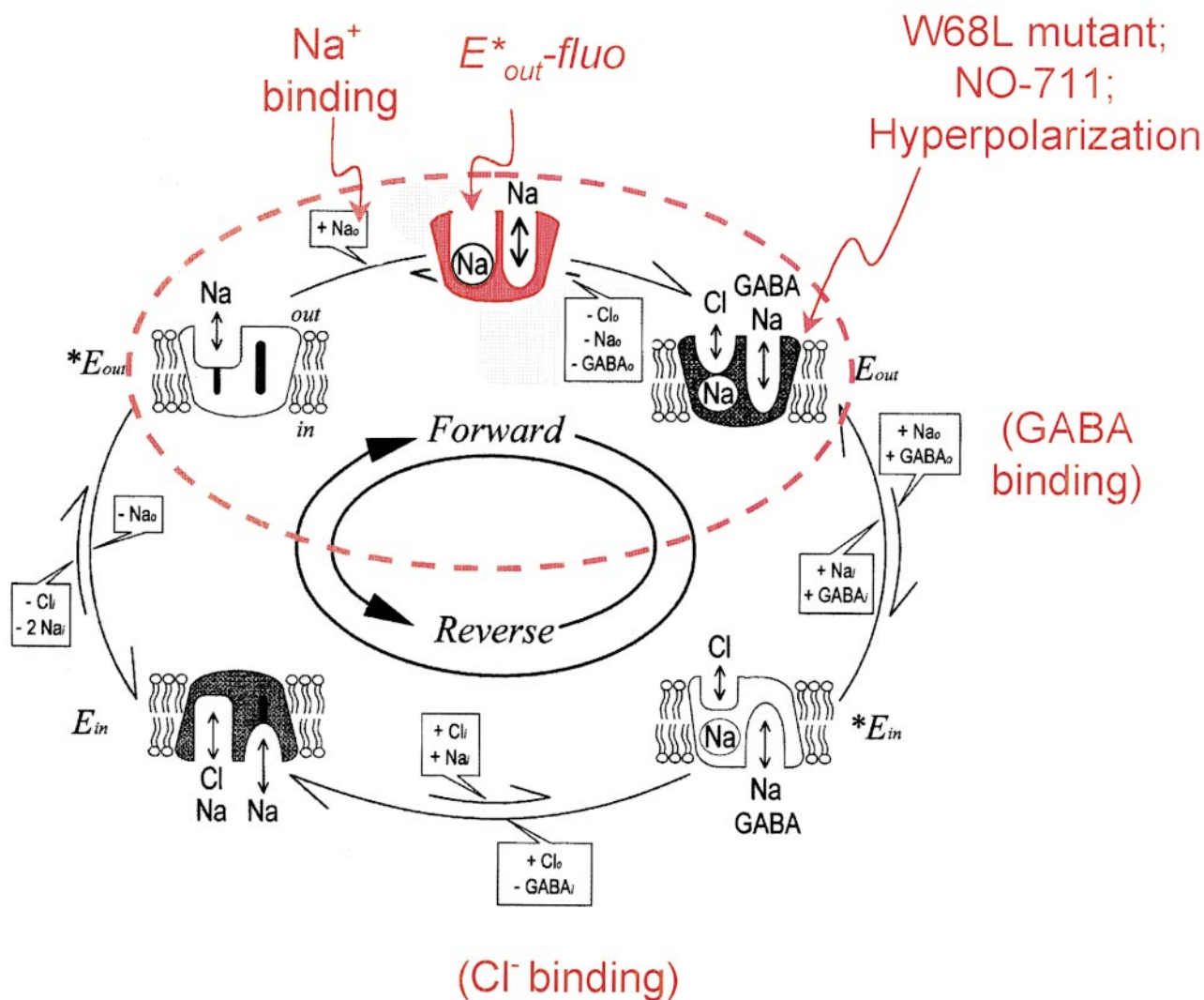
Figure 15. The nature of the fluorescent state: a scheme that fits the available data. The scheme is superimposed on the state diagram accompanying Lu and Hilgemann (1999). The fluorescent state is pictured as a novel state, E^*_{out}-*fluo* between the E^*_{out} and E_{out} states, with characteristics intermediate to these states. Hilgemann and Lu (1999) concluded that the transition from the E^*_{out} to E_{out} is voltage dependent, occludes a Na^+ onto the transporter, and constitutes the major rate-limiting step in the transport cycle. Because the transition is incomplete in the novel state, with Na^+ only partially occluded, the Na^+ concentration dependence and voltage dependence for the transition from E^*_{out} to E^*_{out}-*fluo* are less than those for the complete transition to E_{out}. The dashed oval is drawn to include the novel state and the immediate adjacent stable states; any agents that act within the oval would perturb the fluorescent state strongly enough to be detected in our experiments. The W68L mutant is thought to trap transporter in the state now characterized as E_{out} (Mager et al., 1996), which explains how this mutation eliminates the fluorescence relaxations at most potentials. NO-711 is thought to stabilize the E_{out} states as well (Mager et al., 1996), explaining how it blocks the relaxations. Agents that act outside the oval would perturb the fluorescent state too weakly to be detected in our experiments. The binding of both GABA and Cl^- occur outside the oval, which explains their small effects on the fluorescence relaxations. Therefore, GABA binding and Cl^- binding are shown in parentheses.

gion in GAT1 function was also revealed by other studies. Amino acid residues near Cys74 are proposed to be the Na^+ or Cl^- binding site: this region is most conserved in the Na^+, Cl^--dependent neurotransmitter transporter family, and Arg 69 and Trp 68 in this region, the putative role of which is to interact with ions, are absolutely required for GAT-1 function (Pantanowitz et al., 1993; Kleinberger-Doron and Kanner, 1994; Mager et al., 1996).

That the fluorescence does not directly monitor the GABA-transporter interaction agrees with previous suggestions that the extracellular loops between TM7 and TM8 and between TM11 and TM12 are involved in GABA binding (Tamura et al., 1995). Therefore, it is very possible that the conformational change we detected near Cys74 between TM1 and TM2 does not involve any structural changes in TM7 to TM12 that are induced by GABA binding.

The GAT1 Fluorescence Signal Recalls a Phenomenon at Serotonin Transporters

The serotonin transporter SERT has ~40% sequence similarity to GAT1, and therefore the two transporters presumably share overall structural details. We feel justified in comparing some functional phenomena as well between SERT and GAT1. At SERT, jumps to hyperpolarizing voltages induce the transient activation of a channel-like conducting pathway (Mager et al., 1994). Thus, SERT displays a hyperpolarization-induced conformational change. Several characteristics of this state at SERT resemble those of the state we term E^*_{out}-*fluo* at GAT1. (a) Voltage dependence: both increase with hyperpolarizing voltages with no sign of saturation at membrane voltage of -140 mV. (b) Na^+ dependence: both increase with increasing Na^+ concentration with a Hill coefficient of 1.7–1.8. (c) Cl^- dependence: both are affected by Cl^- to a lesser degree than by Na^+. (d) Substrate dependence: both occur in the absence of the respective neurotransmitter. (e) Time course: both the GAT1 fluorescence signal and the inactivation of the SERT conductance occur on time scale of ~100 ms.

If a state like E^*_{out}-*fluo* does produce the transient resistive current in SERT, then E^*_{out}-*fluo* contains a channel-like pathway in SERT but not in GAT1. Perhaps this partially occluded state, which we have already drawn as extending nearly through the molecule (Fig. 15), is actually open to both sides in SERT. Indeed, several studies suggest that a channel-like pathway also exists in GAT1 (Cammack et al., 1994; Cammack and Schwartz, 1996; Risso et al., 1996). Because channel-like behaviors of neurotransmitter transporters are being investigated intensively (Mager et al., 1994; Cammack and Schwartz, 1996; Sonders et al., 1997; Petersen and DeFelice, 1999; Galli et al., 1998), fluorescence experiments may become a useful tool.

Outlook

Over the past decade, electrophysiological experiments have revealed the existence of several previously unsuspected states at neurotransmitter transporters. We have shown how to conduct fluorescence measurements on a neurotransmitter transporter. We conclude that our measurements monitor a novel conformational state of GAT1, but this state has properties intermediate between those of two known states, and it may resemble a previously described state of SERT. We expect that it will be possible to measure fluorescent signals associated with labeling of other GAT1 residues. We hope that some of these future signals will be larger and therefore more amenable to quantitation.

REFERENCES

Amara, S.G., and M. Kuhar. 1993. Neurotransmitter transporters: recent progress. *Annu. Rev. Neurosci.* 16:73–93.

Baker, O.S., H.P. Larsson, L.M. Mannuzzu and E.Y. Isacoff. 1998. Three transmembrane conformations and sequence-dependent displacement of the S4 domain in *Shaker* K^+ channel gating. *Neuron.* 20:1283–1294.

Bendahan, A., and B.I. Kanner. 1993. Identification of domains of a cloned rat-brain GABA transporter which are not required for its functional expression. *FEBS Lett.* 318:41–44.

Bennett, E.R., and B.I. Kanner. 1997. The membrane topology of GAT-1, a (Na^+ + Cl^-)-coupled γ- aminobutyric acid transporter from rat brain. *J. Biol. Chem.* 272:1203–1210.

Blakely, R.D., H.E. Berson, J.R.T. Fremeau, M.G. Caron, M.M. Peek, H.K. Prince, and C.C. Bradley. 1991. Cloning and expression of a functional serotonin transporter from rat brain. *Nature.* 354:66–70.

Cammack, J.N., S.V. Rakhilin, and E.A. Schwartz. 1994. A GABA transporter operates asymmetrically and with variable stoichiometry. *Neuron.* 13:949–960.

Cammack, J.N., and E.A. Schwartz. 1996. Channel behavior in a GABA transporter. *Proc. Natl. Acad. Sci. USA.* 93:723–727.

Cha, A., and F. Bezanilla. 1997. Characterizing voltage-dependent conformational changes in the *Shaker* K^+ channel with fluorescence. *Neuron.* 19:1127–1140.

Cha, A., and F. Bezanilla. 1998. Structural implications of fluorescence quenching in the *Shaker* K^+ channel. *J. Gen. Physiol.* 112:391–408.

Eskandari, S., E.M. Wright, M. Kreman, D.M. Starace, and G.A. Zampighi. 1998. Structural analysis of cloned plasma membrane proteins by freeze-fracture electron microscopy. *Proc. Natl. Acad. Sci. USA.* 95:11235–11240.

Galli, A., R.D. Blakely, and L.J. DeFelice. 1998. Patch-clamp and amperometric recordings from norepinephrine transporters: channel activity and voltage-dependent uptake. *Proc. Natl. Acad. Sci. USA.* 95:13260–13265.

Golovanevsky, V., and B.I. Kanner. 1999. The reactivity of the γ-aminobutyric acid transporter GAT-1 toward sulfhydryl reagents is conformationally sensitive. Identification of a major target residue. *J. Biol. Chem.* 274:23020–23026.

Guastella, J.G., N. Nelson, H. Nelson, L. Czyzyk, S. Keynan, M.C. Midel, N. Davidson, H.A. Lester, and B. Kanner. 1990. Cloning and expression of a rat brain GABA transporter. *Science.* 249:1303–1306.

Hilgemann, D.W., and C.C. Lu. 1999. GAT1 (GABA:Na^+:Cl^-) cotransport function. Database reconstruction with an alternating access model. *J. Gen. Physiol.* 114:459–476.

Hoffman, B.J., E. Mezey, and M.J. Brownstein. 1991. Cloning of a serotonin transporter affected by antidepressants. *Science.* 254:579–580.

Kanner, B.I. 1978. Solubilization and reconstitution of the γ-aminobutyric acid transporter from rat brain. *FEBS Lett.* 89:47–50.

Kanner, B.I., and A. Bendahan. 1982. Binding order of substrates to the sodium and potassium ion coupled L-glutamic acid transporter from rat brain. *Biochemistry.* 21:6327–6330.

Kleinberger-Doron, N., and B.I. Kanner. 1994. Identification of tryptophan residues critical for the function and targeting of the

γ-aminobutyric acid transporter (subtype A). *J. Biol. Chem.* 269: 3063–3067.

Kluger, R., and W.C. Tsui. 1980. Amino group reactions of the sulfhydryl reagent methyl methanesulfonothioate. Inactivation of d-3-hydroxybutyrate dehydrogenase and reaction with amines in water. *Can. J. Biochem.* 58:629–632.

Kuhar, M.J., M.C. Ritz, and J.W. Boja. 1991. The dopamine hypothesis of the reinforcing properties of cocaine. *Trends Neurosci.* 144: 299–302.

Lester, H.A., Y. Cao, and S. Mager. 1996. Listening to neurotransmitter transporters. *Neuron.* 17:807–810.

Loo, D.D., B.A. Hirayama, E.M. Gallardo, J.T. Lam, E. Turk, and E.M. Wright. 1998. Conformational changes couple Na^+ and glucose transport. *Proc. Natl. Acad. Sci. USA.* 95:7789–7794.

Loots, E., and E.Y. Isacoff. 1998. Protein rearrangements underlying slow inactivation of the *Shaker* K^+ channel. *J. Gen. Physiol.* 112: 377–389.

Lu, C.C., and D.W. Hilgemann. 1999a. GAT1 (GABA:Na^+:Cl^-) cotransport function. Kinetic studies in giant *Xenopus* oocyte membrane patches. *J. Gen. Physiol.* 114:445–458.

Lu, C.C., and D.W. Hilgemann. 1999b. GAT1 (GABA:Na^+:Cl^-) cotransport function. Steady state studies in giant *Xenopus* oocyte membrane patches. *J. Gen. Physiol.* 114:429–444.

Lu, C.-C., A. Kabakov, V.S. Markin, S. Mager, A. Frazier, and D.W. Hilgemann. 1996. Membrane transport mechanisms probed by capacitance measurements with megahertz voltage clamp. *Proc. Natl. Acad. Sci.USA.* 92:11220–11224.

Mabjeesh, N.J., and B.I. Kanner. 1992. Neither amino nor carboxyl termini are required for function of the sodium- and chloride-coupled γ-aminobutyric acid transporter from rat brain. *J. Biol. Chem.* 267:2563–2568.

Mager, S., Y. Cao, and H.A. Lester. 1998. Measurement of transient currents from neurotransmitter transporters expressed in *Xenopus* oocytes. *Methods Enzymol.* 296:551–566.

Mager, S., N. Kleinberger-Doron, G.I. Keshet, N. Davidson, B.I. Kanner, and H.A. Lester. 1996. Ion binding and permeation at the GABA transporter GAT1. *J. Neurosci.* 16:5405–5414.

Mager, S., C. Min, D.J. Henry, C. Chavkin, B.J. Hoffman, N. Davidson, and H.A. Lester. 1994. Conducting states of a mammalian serotonin transporter. *Neuron.* 12:845–859.

Mager, S., J. Naeve, M. Quick, J. Guastella, N. Davidson, and H.A. Lester. 1993. Steady states, charge movements, and rates for a cloned GABA transporter expressed in *Xenopus* oocytes. *Neuron.* 10:177–188.

Mannuzzu, L.M., M.M. Moronne, and E.Y. Isacoff. 1996. Direct physical measure of conformational rearrangement underlying potassium channel gating. *Science.* 271:213–216.

Means, G., and R.E. Feeney. 1971. Chemical Modification of Proteins. Holden-Day, Inc., San Francisco, CA. 105–114.

Pacholczyk, T., R.D. Blakely, and S.G. Amara. 1991. Expression cloning of a cocaine-sensitive and antidepressant-sensitive human noradrenaline transporter. *Nature.* 350:350–354.

Pantanowitz, S., A. Bandahan, and B.I. Kanner. 1993. Only one of the charged amino-acids located in the transmembrane α-helices of the γ-aminobutyric-acid transporter (subtype-A) is essential for its activity. *J. Biol. Chem.* 286:3222–3225.

Pastuszko, A., D.F. Wilson, and M. Erecinska. 1982. Energetics of γ-aminobutyrate transport in rat brain synaptosomes. *J. Biol. Chem.* 257:7514–7519.

Penado, K.M., G. Rudnick, and M.M. Stephan. 1998. Critical amino acid residues in transmembrane span 7 of the serotonin transporter identified by random mutagenesis. *J. Biol. Chem.* 273: 28098–28106.

Petersen, C.I., and L.J. DeFelice. 1999. Ionic interactions in the *Drosophila* serotonin transporter identify it as a serotonin channel. *Nat. Neurosci.* 2:605–610.

Quick, M.W., and H.A. Lester. 1994. Methods for expression of excitability proteins in *Xenopus* oocytes. *Methods Neurosci.* 19:261–279.

Radian, R., and B.I. Kanner. 1983. Stoichiometry of sodium- and chloride-coupled γ-aminobutyric acid transport by synaptic plasma membrane vesicles isolated from rat brain. *Biochemistry.* 22:142–168.

Radian, R., and B.I. Kanner. 1985. Reconstitution and purification of the sodium- and chloride-coupled g-aminobutyric acid transporter from rat brain. *J. Biol. Chem.* 260:11859–11865.

Risso, S., L.J. DeFelice, and R.D. Blakely. 1996. Sodium-dependent GABA-induced currents in GAT1-transfected HeLa cells. *J. Physiol.* 490:691–702.

Rudnick, G. 1977. Active transport of 5-hydroxytryptamine in plasma membrane vesicles isolated from human blood platelets. *J. Biol. Chem.* 252:2170–2174.

Rudnick, G., and P.J. Nelson. 1978. Platelet 5-hydroxytryptamine transport, an electroneutral mechanism coupled to potassium. *Biochemistry.* 17:4739–4742.

Shimada, S., S. Kitayama, C.L. Lin, A. Patel, E. Nanthakumar, M. Kuhar, and G. Uhl. 1991. Cloning and expression of a cocaine-sensitive dopamine transporter complementary-DNA. *Science.* 254:576–578.

Siegel, M.S., and E.Y. Isacoff. 1997. A genetically encoded optical probe of membrane voltage. *Neuron.* 19:735–741.

Sonders, M., S.-J. Zhu, N. Zahniser, M. Kavanaugh, and S. Amara. 1997. Multiple ionic conductances of the human dopamine transporter: the actions of dopamine and psychostimulants. *J. Neurosci.* 17:960–974.

Stephan, M., G. Kamdar, G. Rudnick, and K. Penado. 1999. A functional link between transmembrane span 7 and extracellular loop 1 of the serotonin transporter: effects of Na^+, Li^+, and methansulfonate reagents. *Soc. Neurosci. Abstr.* 25:1699.

Su, A., S. Mager, S.L. Mayo, and H.A. Lester. 1996. A multi-substrate single-file model for ion-coupled transporters. *Biophys. J.* 70:762–777.

Tamura, S., H. Nelson, A. Tamura, and N. Nelson. 1995. Short external loops as potential substrate binding site of γ-aminobutyric acid transporters. *J. Biol. Chem.* 270:28712–28715.

Usdin, T.B., E. Mezey, C. Chen, M.J. Brownstein, and B.J. Hoffman. 1991. Cloning of the cocaine-sensitive bovine dopamine transporter. *Proc. Natl. Acad. Sci. USA.* 88:11168–11171.

Yu, N., Y. Cao, S. Mager, and H.A. Lester. 1998. Topological localization of cysteine 74 in the GABA transporter, GAT1, and its importance in ion binding and permeation. *FEBS Lett.* 426:174–178.